

V745 Cassiopeia: an interacting young massive binary in a multiple star system^{*}

Ö. Çakırlı^{1†}, C. Ibanoglu¹, E. Sipahi¹,

¹*Ege University, Science Faculty, Astronomy and Space Sciences Dept., 35100 Bornova, İzmir, Turkey*

25 July 2018

ABSTRACT

We present spectroscopic observations of the massive early type system V745 Cas, embedded in a multiple star system. The brightest star of the system is the eclipsing binary V745 Cas with an orbital period of 1.41 days. The radial velocities of both components and light curves obtained by *INTEGRAL* and *Hipparcos* missions were analysed. The components of V745 Cas are shown to be a B0 V primary with a mass $M_p=18.31\pm 0.51 M_\odot$ and radius $R_p=6.94\pm 0.07 R_\odot$ and a B(1-2) V secondary with a mass $M_s=10.47\pm 0.28 M_\odot$ and radius $R_s=5.35\pm 0.05 R_\odot$. Our analysis shows that both components fill their corresponding *Roche* lobes, indicating double contact configuration. Using the UBVJHK magnitudes and interstellar absorption we estimated the mean distance to the system as 1700 ± 50 pc. The locations of the component stars in the mass-luminosity, mass-radius, effective temperature-mass and surface gravity-mass are in agreement with those of the main-sequence massive stars. We also obtained *UBV* photometry of the three visual companions and we estimate that all are B-type stars based upon their de-reddened colours. We suspect that this multiple system is probably a member of the Cas OB4 association in the *Perseus* arm of the *Galaxy*.

Key words: stars: binaries: eclipsing – stars: fundamental parameters – stars: binaries: spectroscopic – stars:

^{*} Based on the data obtained at TÜBİTAK National Observatory

[†] e-mail: omur.cakirli@gmail.com

1 INTRODUCTION

The number of eclipsing massive binary stars, having $M > 9 M_{\odot}$, is small in comparison to lower mass systems (Gies (2003), Hilditch et al. (2005), Massey et al. (2012), Moe & Di Stefano (2013), Sana et al. (2013)). Massive stars are usually formed in OB associations. It is well known that massive stars evolve faster and are of interest as progenitors of neutron stars and black holes. The evolutionary paths of massive binaries depend on processes related to mass transfer between the components and mass loss via stellar wind from one or both components. Consequently, in order to better understand the physics of binary systems and test the predictions of theoretical models, it is thus important to quantitatively analyse the properties of massive binary systems with well-constrained orbital parameters. In this context studies of the rare early B-type massive stars has major highlights for understanding formation mechanism and evolution of massive binaries. Torres et al. (2010) collected accurate fundamental parameters, for the 95 double-lined detached binary systems. The number of binary systems with masses and radii determined to an accuracy of better than 3% decreases towards the massive stars. The number of systems with at least one component more massive than $9 M_{\odot}$ does not exceed ten (Torres et al. 2010). Therefore, we initiated a spectroscopic study for the close binary systems which include high mass stars located in the upper left-hand corner of the Hertzsprung-Russell diagram.

V745 Cas (HD1810, HIP 1805, WDS J00229+6214AB, $V=8.11$, $B-V=0.06$) is the brightest star of a multiple star system. WDS J00229+6214 consists of five stars. The angular distances of B, C, D and E from the brightest star A are given in the Washington Double Stars Catalog¹ as 9.5, 23.2, 44.9 and 57.8 arcseconds, respectively. The visual apparent magnitudes of the stars A, B, C, D, and E are also estimated as 8.12, 11.13, 10.8, 12.14 and 12.85 mag. Despite its relative brightness, V745 Cas has not been comprehensively studied yet. The first spectral classification for V745 Cas (B0 IV) has been dating back to Morgan, Whitford, & Code (1953). Haug (1970) gives $V=8^m.19$, $(B-V)=0^m.08$, while Guetter (1974) gives $V=8^m.16$, $(U-B)=-0^m.83$ and $(B-V)=0^m.05$. Its radial velocity, averaging $V=-50 \text{ km s}^{-1}$, was found to be variable by Sanford & Merrill (1938), Wilson (1953), Petrie & Pearce (1961), and Evans (1967). V745 Cas is listed in the optical pairs by Meisel (1968) who estimated the spectral types of the A and B components as B0 IVp and A9 V with a magnitude difference of 1.5 mag. Reed (2003) estimates visual magnitude and color indices of the A component as $8^m.19$, $(U-B)=-0^m.79$ and $(B-V)=0^m.08$.

The light variability of V745 Cas has been discovered thanks to the Hipparcos satellite mission

¹ <http://ad.usno.navy.mil/wds/>

(Perryman et al. 1997). The H_p magnitudes at the maximum and minimum light of the brightest component A of the multiple system are given as $8^m.063$ and $8^m.164$, i.e. a magnitude variation by about $0^m.10$. The light curve was classified as a W UMa-type eclipsing binary according to the criteria of the General Catalogue of variable Stars, with an orbital period of 1.41057 days from visual inspection of light variation. The Hipparcos' light curve shows that the depths of the eclipses are nearly identical. Kazarovets et al. (1999) designated it as V745 Cas in the 74th Name-list of Variable Stars, and classified it as an EB.

V745 Cas is located in the sky in the vicinity of the Cas OB4 and Cas OB14 associations. While the star was not included as a member of Cas OB4 association by Humphreys (1978) and Garmany & Stencel (1992), it is included into the list of members of Cas OB4 by Mel'nik & Efremov (1995) and Mel'nik & Dambis (2009). These associations are located in the Perseus arm of the Galaxy. Many estimates have been made about their distances to the Sun. These estimates indicate that the Cas OB14 association is closer to the sun having a distance of about 1 kpc, which is less than half the distance of Cas OB4.

This paper is organized as follows. We present new spectroscopic observations and radial velocities of both components of the eclipsing pair. By analysing the *INTEGRAL* and Hipparcos missions' light curves and the new radial velocities we obtain orbital parameters for the stars. Combining the results of these analyses we obtain absolute physical parameters of both components. In addition, we conclude with a discussion of the system's evolutionary status.

2 SPECTROSCOPIC OBSERVATIONS AND DATA REDUCTIONS

Optical spectroscopic observations of V745 Cas were obtained with the Turkish Faint Object Spectrograph Camera (TFOSC) attached to the 1.5 m telescope from January 2 to August 28, 2012, under good seeing conditions. Further details on the telescope and the spectrograph can be found at <http://www.tug.tubitak.gov.tr>. The wavelength coverage of each spectrum was 4000-9000 Å in 12 orders, with a resolving power of $\lambda/\Delta\lambda \sim 7\,000$ at 6563 Å and an average signal-to-noise ratio (S/N) was ~ 120 . We also obtained high S/N spectra of early type standard stars 1 Cas (B0.5 IV), HR 153 (B2 IV), τ Her (B5 IV), 21 Peg (B9.5 V), and α Lyr (A0 V) for use as templates in derivation of the radial velocities.

The data reduction was performed using the echelle task of IRAF ² ECHELLE PACKAGE

² IRAF is distributed by the *National Optical Astronomy* Observatory, which is operated by the Association of Universities for Research in Astronomy, Inc. (AURA), under cooperative agreement with the National Science Foundation

(Simkin 1974) following the standard steps: background subtraction, division by a flat-field spectrum given by a halogen lamp, wavelength calibration using the emission lines of a Fe-Ar lamp, and normalization to the continuum through a polynomial fit. Heliocentric corrections were computed using the IRAF RVSAO.BCVCORR routine and were taken into account in the subsequent radial velocity determination.

2.1 Radial Velocities

Radial velocities of the components were measured by cross-correlation with the FXCOR task in IRAF (Simkin (1974), Tonry & Davis (1979)). The standard stars with known radial velocities, given in previous section, were used as templates. The standard stars' spectra were synthetically broadened by convolution with the broadening function of Gray (1992). The cross-correlation with the standard star 1 Cas gave the best result. The spectra showed two distinct cross-correlation peaks at the quadratures, one for each component of the binary. Since the two peaks appear blended, a double *Gaussian* fit was applied to the combined profile using *de-blend* function in the task.

The cross-correlation technique was applied to four wavelength regions with well-defined absorption lines of the primary and secondary components. These regions include He I lines at $\lambda 4471$ (in the 9th order), $\lambda 5876$ (in the 3rd order), $\lambda 6678$ (in the 3rd order), and $\lambda 7065$ (in the 2nd order) dominant in early B-type stars. Here we used as weights the inverse of the variance of the radial velocity measurements in each order, as reported by FXCOR. We have been able to measure radial velocities of both components with a precision better than 10 km s^{-1} extracted from the FXCOR. The *Balmer* lines were not used in the measurements of radial velocities due to their extremely Stark-broadened and rotationally broadened profiles.

The heliocentric radial velocities for the primary (V_p) and the secondary (V_s) components are listed in Table 1, along with the dates of observations and the corresponding orbital phases computed with the new ephemeris given in Sect. 2.1. The velocities in this table have been corrected to the heliocentric reference system by adopting a radial velocity value for the template stars. The radial velocities are plotted against the orbital phase in Fig. 1 where the filled squares correspond to the primary and the empty squares to the secondary star. Examination of the *Integral – OMC* and *Hipparcos* light curves shows no evidence for any eccentricity in the orbit of the system. Therefore, we have started with a circular orbit and analysed the RVs using the RVSIM software program (Kane, Schneider, & Ge 2007). The results of the common center-of-velocity analysis of

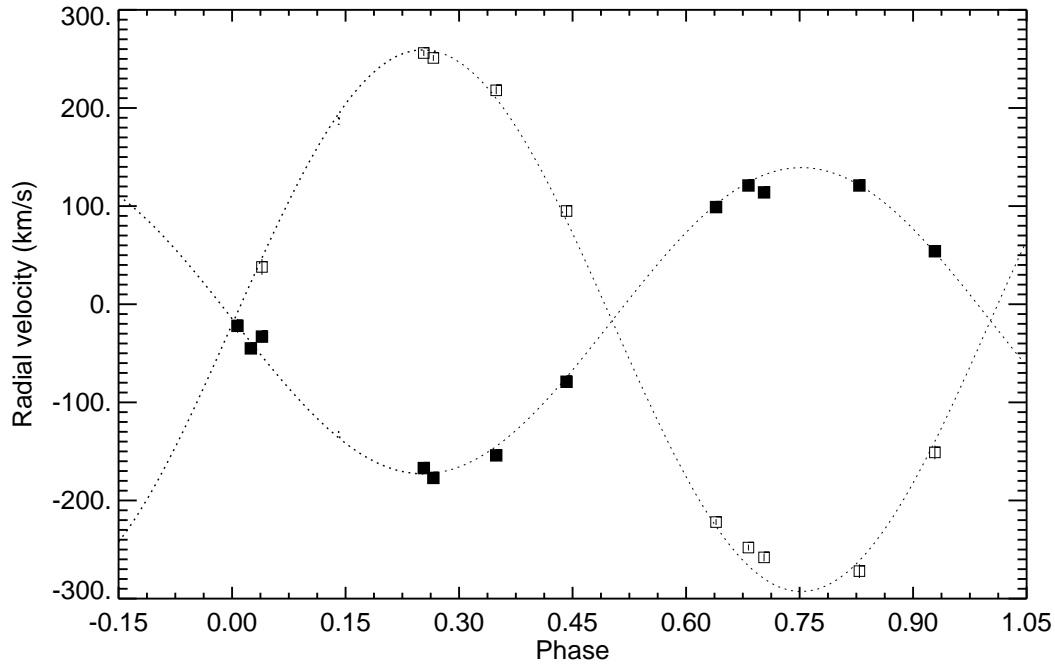


Figure 1. Radial velocities for the components of V745 Cas. Symbols with error bars (masked by the symbol size) show the radial velocity measurements for the components of the system (primary: filled squares, secondary: open squares).

Table 1. Heliocentric radial velocities of V745 Cas. The columns give the heliocentric Julian date, orbital phase and the radial velocities of the two components with the corresponding standard deviations.

HJD 2400000+	Phase	Star 1		Star 2	
		V_p	σ	V_s	σ
55929.4430	0.4420	-79	5	95	6
55930.2400	0.0071	-22	7	—	9
56130.5869	0.0395	-33	6	38	8
56131.5227	0.7030	114	3	-258	4
56132.4341	0.3491	-154	4	218	4
56133.3873	0.0248	-45	5	—	6
56134.5216	0.8290	121	4	-272	7
56136.5308	0.2534	-167	2	256	3
56137.4836	0.9288	54	6	-151	7
56162.4659	0.6396	99	2	-222	3
56162.5262	0.6824	121	2	-248	3
56167.5812	0.2660	-177	3	251	3

the radial velocities are presented in Table 2. The best fit was obtained for a circular orbit with a mass-ratio of $q = \frac{M_2}{M_1} = 0.571 \pm 0.010$. The dotted lines in Fig. 1 show the computed curves.

Table 2. Results of the radial velocity analysis for V745 Cas

Parameter	Primary	Secondary
K (km s $^{-1}$)	156 ± 2	273 ± 3
V_γ (km s $^{-1}$)	-16 ± 2	-16 ± 2
Average O-C (km s $^{-1}$)	4	3
$M \sin^3 i$ (M_\odot)	7.34 ± 0.20	4.20 ± 0.11
$a \sin i$ (R_\odot)	4.348 ± 0.056	7.608 ± 0.083

3 SPECTRAL ANALYSIS

Fundamental stellar parameters, such as projected rotational velocity ($v \sin i$), spectral type (Sp), luminosity class, effective temperature (T_{eff}), surface gravity ($\log g$), and metallicity ($[Fe/H]$) may be determined from the mid-resolution optical spectroscopy.

3.1 The projected rotational velocities

Projected rotational velocities of early-type stars were determined usually by means of various methods: the full-width-at-half-maximum (FWHM) method (Abt et al. 2002), the goodness-of-fit (GOF) method (Conti & Ebbets 1977), the cross-correlation-function (CCF) method (Penny 1996), the Fourier transform (FT) method (Gray 1976), and the *iacob–broad* method (Simón-Díaz & Herrero 2014), based on a combination of GOF and FT methodologies.

We used the CCF -method for measurement of the individual projected rotational velocities ($v \sin i$) of the component stars. The rotational velocities of the components were obtained by measuring the full-width-at-half-maximum (FWHM) of the CCFs in five high-S/N spectra of the components acquired close to the quadratures, where the spectral lines have the largest Doppler-shift. The He I lines at $\lambda\lambda 4471$, 6678 and 7065 lines were selected. The CCFs were used for the determination of $v \sin i$ through a calibration of the FWHM of the CCF peak as a function of the $v \sin i$ of artificially broadened spectra of slowly rotating standard star (21 Peg, $v \sin i \simeq 14 \text{ km s}^{-1}$, e.g., Royer et al. (2002)) acquired with the same set up and in the same observing night as the target. The limb darkening coefficient was fixed at the theoretically predicted values of 0.42 for both stars (van Hamme 1993). We calibrated the relationship between the CCF Gaussian width and $v \sin i$ using the Conti & Ebbets (1977) data sample. This analysis yielded projected rotational velocities for the components of V745 Cas as $V_p \sin i = 171 \text{ km s}^{-1}$, and $V_s \sin i = 151 \text{ km s}^{-1}$. The mean deviations were 4 and 8 km s^{-1} , for the primary and secondary, respectively, between the measured velocities for different lines.

3.2 The spectral classification

Spectral types of the components were first estimated by comparison both with our standard stars' spectra and also with templates taken from the Valdes et al. (2004) *Indo–U.S. Library of Coude Feed Stellar S* (with a resolving power of about $R=3600$) that are representative of stars with various metallicities, spectral types from late-O type to early-A, and luminosity classes V, IV, and III.

We have performed a spectral classification for the components of the system using COMPO2,

an IDL (INTERACTIVE DATA LANGUAGE RSI) code for the analysis of the spectra of SB2 systems written by Frasca et al. (2006). This code, similar to the SYNTHE code (Kurucz & Avrett 1981), was adapted to the TFOSC spectra of the binary systems. This code searches for the best combination of two standard-star spectra able to reproduce the observed spectrum of the system. We give, as input parameters, the radial velocities and projected rotational velocities $v \sin i$ of the two components, which were already derived. The code then finds, for the selected spectral region, the spectral types and fractional flux contributions that better reproduce the observed spectrum, i.e. which minimize the residuals in the collection of difference (observed – constructed) spectra.

The atmospheric parameters of the reference stars given by Valdes et al. (2004) were recently revised by Wu et al. (2011). For this task we selected about 200 single-star' spectra spanning the ranges of expected atmospheric parameters, which means that we have searched for the best combination of spectra among 39204 possibilities per each spectrum.

The observed spectra of V745 Cas around the $\lambda\lambda 4471$, and 6678 spectral lines were best represented by combination of the spectra of HD 34816 (B0.5 V, $\log g=3.91$) and HD 184915 (B1.5 III, $\log g=3.40$). We have derived the spectral types for the primary and secondary component of V745 Cas as B(0 ± 0.5) V and B(1.5 ± 0.5) III, respectively. The atmospheric parameters obtained by the code are presented in Table 3. The observed spectra of V745 Cas at nearly quadratures around the He I lines at $\lambda\lambda 4471$, and 6678 are compared with the combination of two single-star' spectra in Fig. 2.

This result can be confirmed using the ratios of equivalent widths of He I 4471 and He II 4541 lines. Spectral lines of the components are well separated at the quadratures of the eclipsing pair. We measured equivalent widths (EW) of the primary star He I 4471 and He II 4541 lines for estimating **its spectral type**. The average logarithmic ratio of the equivalent widths (EW) of the primary is about 1.19 ± 0.17 , which corresponds to a B0 type star (van der Hucht 1996). The luminosity criterion based on the logarithm of the ratio of the line strengths of Si IV 4088 and He I 4143 (Conti, Garmany & Massey 1986; van der Hucht 1996) yields -1.07 ± 0.05 . This value corresponds to main-sequence (luminosity class V) stars.

Further support for this classification comes from the photometry of V745 Cas available in the literature. The visual apparent magnitude and colour indices were given by Guetter (1974) as $V=8^m.16$, $(U - B)=-0^m.83$ and $(B - V)=0^m.05$ with an uncertainty of ± 0.01 mag. The quantity $Q=(U - B)-(E_{(U-B)}/(E_{(B-V)}))(B - V)$ is independent of interstellar extinction. The average value of the ratio $(E_{(U-B)}/(E_{(B-V)}))$ is 0.72 ± 0.03 (Johnson & Morgan (1953); Hovhannessian (2004)). We compute the reddening-free index from the data of Guetter (1974) as $Q=-0.866\pm 0.014$. The

Table 3. Spectral types, effective temperatures, surface gravities, and rotational velocities of each star estimated from the spectra of V745 Cas.

Parameter	V745 Cas	
	Primary	Secondary
Spectral type	B(0±0.5)V	B(1.5±0.5)III
T_{eff} (K)	30 000±880	25 600±1 050
$\log g$ (cgs)	3.91±0.00	3.40±0.00
$V \sin i$ (km s ⁻¹)	171±4	151±8

Q – values were calculated by Hovhannessian (2004) beginning from O8 to G2 spectral types for the luminosity classes between main-sequence and supergiants. The $Q-S_p$ calibration yields an approximate spectral type of the system as B0 with a range from O9 to B1. The spectral classification from the spectra and photometric indices are quite consistent.

In addition, infrared colors $J-H=-0.057\pm0.064$, $H-K=0.015\pm0.062$ mag are given in the 2MASS catalog (Cutri et al. 2003). These indices confirm spectral classifications made by spectra and wide-band photometric indices. A preliminary analysis of the light curve (see Section 4.3) yields light ratio of 0.43 for the V-passband. This light ratio, the observed colours and the intrinsic colour of the primary star of $(B-V)_0=-0.30\pm0.01$ (Drilling & Landolt 2000) allow us to estimate an intrinsic composite colour of $(B-V)_0=-0.29\pm0.01$. Thus, the interstellar reddening of $E_{(B-V)}=0.34\pm0.01$ mag is estimated for the system.

4 ANALYSES OF THE LIGHT CURVES

4.1 Light Curve Constraints

The first photometric observations of V745 Cas were made by the Hipparcos mission and 144 H_p magnitudes were listed by van Leeuwen (2007). These magnitudes were obtained in a time interval of about three years. The average accuracy of the Hipparcos data was given as $\sigma_{H_p} \sim 0.01$ mag. The light variation from peak-to-peak is about 0.12 mag. However, we have estimated a scatter of about 0.022 mag at the maxima and within the primary minimum. The scatter at the secondary eclipse is slightly larger, amounting to 0.028 mag.

The second set of photometric observations were made by the *International Gamma – Ray Astrophysics Laboratory (INTEGRAL)* mission (Alfonso-Garzón et al. 2013)]. The *Integral-OMC* database contains light curves for many previously unknown variable stars. We extracted the V-passband light curve for V745 Cas (*Integral – OMC* 4019000053) from this catalog. The *INTEGRAL* data are consisting of 1 980 Johnson’s V-passband magnitudes. Domingo et al. (2003) estimate an average accuracy of about 0.006 mag for objects of $V=12$ mag.

The 1 980 photometric measurements of *Integral*, including eclipses, permit determination

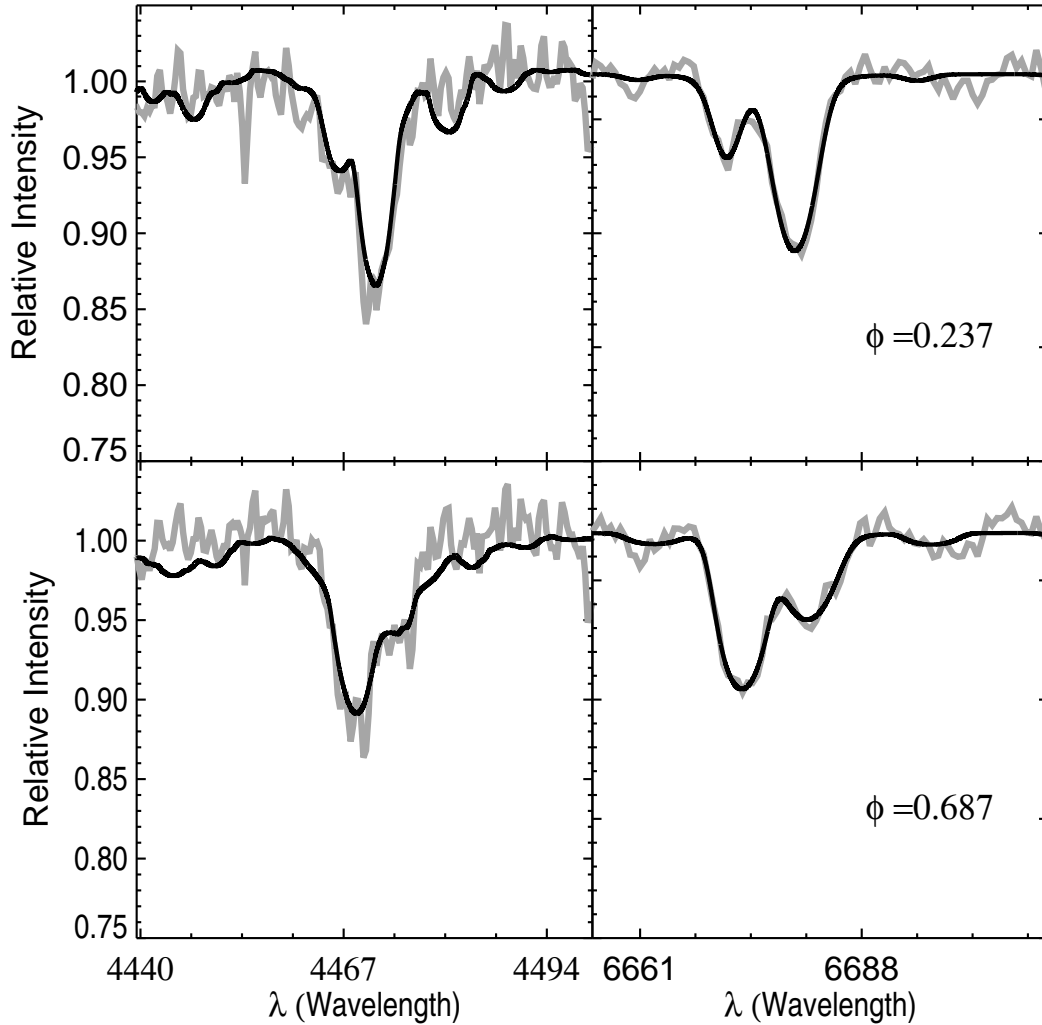


Figure 2. Comparison between the observed spectra of V745 Cas obtained near quadratures and the best-fitting spectra around He I $\lambda 4471$ (left panel) and the $\lambda 6678$ lines (right panel). The deeper lines indicate the primary and the shallow ones the secondary star.

of the time of mid-primary eclipse and the orbital period of the system. A periodogram analysis, e.g. PERIOD04 (Lenz & Breger 2005), has been applied to the data obtained by *INTEGRAL* mission. We determine following ephemeris

$$MinI(HJD) = 2\,455\,222.1234(2) + 1^d.410571(7) \times E \quad (1)$$

where the standard deviations in the last significant digits are given in parentheses. However, Alfonso-Garzón et al. (2012) determined an orbital period of 1.4106019 d, which is slightly longer than we found. Periodogram analysis indicates that there is a light variation with a second period of about 0.1659 ± 0.0007 days (approximately 4 h) having a peak-to-peak amplitude of about 0.014 mag. If this light variation really exists it may originate from intrinsic variation of one or both stars. The spectral types of the components are similar to those of β Cephei type pulsating stars. Therefore such intrinsic variation may be expected from the components of V745 Cas.

Table 4. Results of the analyses of the light curve for V745 Cas.

Parameter	Mode 2	Mode 3	Mode 4	Mode 5	Mode 6
i°	43.65 ± 0.03	47.30 ± 0.32	44.08 ± 0.12	48.07 ± 0.20	47.51 ± 0.22
T_{eff1} (K)	30 000[Fix]	30 000[Fix]	30 000[Fix]	30 000[Fix]	30 000[Fix]
T_{eff2} (K)	$14\,210 \pm 235$	$25\,350 \pm 315$	$17\,580 \pm 320$	$25\,350 \pm 301$	$25\,540 \pm 300$
Ω_1	3.0572 ± 0.0079	3.0098 ± 0.0036	3.0099	3.0181 ± 0.0067	3.0099 ± 0.019
Ω_2	2.8105 ± 0.0040	3.0080 ± 0.019	2.8908 ± 0.0081	3.0099 ± 0.019	3.0099 ± 0.019
r_1	0.4202 ± 0.0015	0.4285 ± 0.0007	0.4281 ± 0.0016	0.4251 ± 0.0013	0.4281 ± 0.0016
r_2	0.3816 ± 0.0012	0.3301 ± 0.0007	0.3572 ± 0.0021	0.3297 ± 0.0015	0.3297 ± 0.0015
$\frac{L_1}{(L_1+L_2)}$	0.8274 ± 0.0033	0.7033 ± 0.0047	0.7951 ± 0.0048	0.7002 ± 0.0047	0.6979 ± 0.0046
$\sum (O - C)^2$	1.0242	1.0484	1.0353	1.0486	1.0477

However, existence of such a variation should be checked by precise multi-passband photometric observations.

We have measured the magnitude difference between the A and B components of the visual pair as 3.13 mag (see Chapter 4) in the V-passband. This difference is slightly larger than the difference of 3.01 mag given by the *WDS catalogue*. Since the INTEGRAL Optical Monitoring Camera has an angular resolution of about 23 arcsec its photometric data cover the light contribution of the component B. Light contribution of the component B to the total light has been calculated as 0.053 which slightly affects the observed magnitudes. Therefore we subtracted the light contribution of component B from all the measured magnitudes. On the other hand the H_p magnitudes measured by the *Hipparcos* mission were transformed to the Johnson's V-passband using the transformation coefficients given by Harmanec (1998). Then both data sets were combined for a simultaneous analysis. All available photometric data are phased and plotted in Fig. 3, where the open circles represent the Hipparcos data. It is clear from Fig. 3 that V745 Cas is an eclipsing binary, with a W UMa type light curve that is dominated by variations due to tidal distortion.

In order to model the photometric light curve, we have used the computer programme *PHOEBE* (PHysics Of Eclipsing BinariEs) developed by Prša & Zwitter (2005). This program is an implementation of the Wilson-Devinney (hereafter WD) binary star code (Wilson & Devinney 1971). The Roche geometry, sensitive to the mass-ratio, is used to represent the tidal deformation of the two stars. One of the main difficulties in this modelling is determination of effective temperature of the primary star and the mass-ratio of the system. Effective temperatures of both stars could already be determined from the spectra. In addition the mass-ratio, which is the second key-parameter for the modelling, was also obtained from the radial velocities of the stars.

Linear limb-darkening coefficients were interpolated from the tables of van Hamme (1993). They are updated at every iteration by *PHOEBE*. The gravity-brightening coefficients $g_1=g_2=1.0$ and albedos $A_1=A_2=1.0$ were fixed for both components, as appropriate for stars with radiative atmospheres.

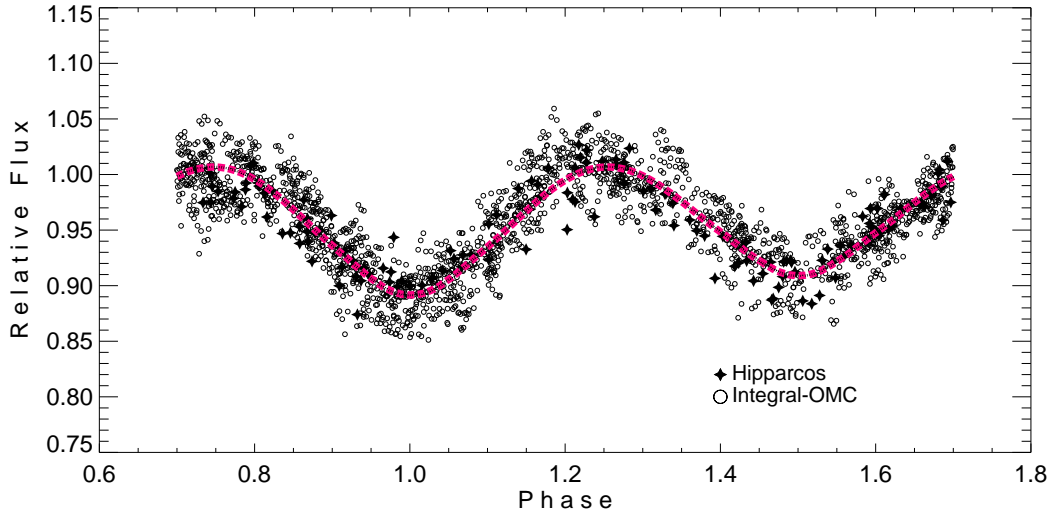


Figure 3. V-passband light curve constructed from the *INTEGRAL* (empty circles) and *Hipparcos* (filled stars) photometric data of V745 Cas. The continuous and dashed lines show the best-fit models obtained by the WD code using the Mode 6 and Mode 3, respectively.

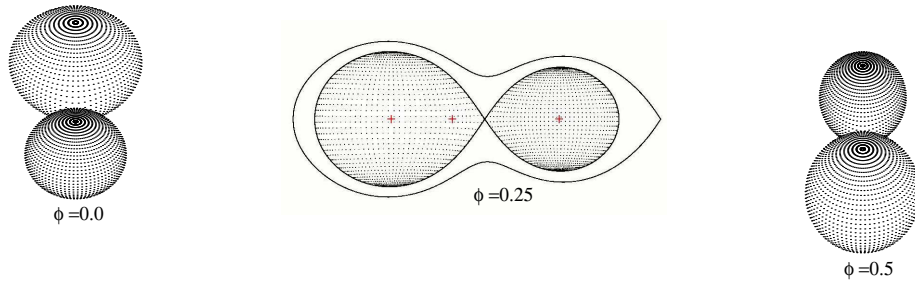


Figure 4. Equipotential structure of V745 Cas corresponding to the solution of the light curve using Mode 6 at the mid-primary (left) and mid-secondary (right) eclipses. Comparison with the Roche lobes is shown in the middle.

4.2 Light Curve Solutions

We started with the *Mode – 2* of the Wilson-Devinney code, referring to the detached Algols for the analysis of light curves as described by Wilson (2006). The adjustable parameters in the light curve fitting were the orbital inclination (i), the effective temperature of the secondary star (T_{eff2}), the potentials (Ω_1 and Ω_2), the luminosity of the primary (L_1), and the zero-epoch offset. The parameters of the solution are tabulated as *Mode – 2* in Table 4. The effective temperature, fractional luminosity and fractional radius of the secondary are about 14 000 K, 0.17, and 0.38, respectively. The effective temperature and fractional luminosity are too small, nearly half, when compared to the values estimated from the spectra. We obtain an inclination of about 43.7 degrees which yields masses of about 22 and 13 M_{\odot} for the primary and secondary star respectively. When the volumes of the stars are compared with their corresponding Roche lobes we see that while the

primary fills up its lobe the secondary star overflows its lobe. Since the configuration is inconsistent with the detached assumption the results of the analysis are taken to be unacceptable.

Next, we tried *Mode* – 3 (for overcontact systems, the stars are in geometrical contact without being in thermal contact). The adjustable parameters were i , T_{eff2} , and L_1 . The results of the analysis are presented in the third column of Table 4. Analysis with this mode yields higher i , T_{eff2} , and L_2 but lower fractional radius for the secondary star. Although the sum of residuals squared is slightly larger from that obtained in *Mode* – 2 these results are in agreement with those obtained from the spectra. However, comparison with the Roche lobes shows that both components are in contact with their inner Roche lobes, which is inconsistent with the assumption of overcontact configuration. In other words, the solution clearly reveals a fill-out factor $f=(\Omega_{in} - \Omega)/(\Omega_{in} - \Omega_{out})=0$, corresponding to the contact configuration.

The results of the analyses using *Mode*–4 (primary star fills its lobe) and *Mode*–5 (secondary star fills its lobe) were given in the fourth and fifth columns of Table 4. The analysis with *Mode*–4 gives similar results as *Mode* – 2, but slightly larger $\sum(O - C)^2$. While the primary component fills its lobe the secondary overfills its lobe which is inconsistent with the *a priori* assumption. The analysis under the assumption of *Mode* – 5 gives the parameters which are very close to those obtained by the *Mode* – 3 solution. However, comparison with the Roche lobes shows that both components are just in contact with their corresponding Roche lobes.

Comparison with the Roche lobes points out double contact configuration. Therefore, we applied *Mode* – 6 (for double contact systems) for the analysis of the observed light curve. The results of this analysis are given in the last column of Table 4. The uncertainties assigned to the adjusted parameters are the internal errors provided directly by the code. While the sum of residuals squared is slightly larger than those obtained by *Mode* – 2 and *Mode* – 4, it is slightly smaller than those obtained by *Mode* – 3 and *Mode* – 5. However, it should be noted that the solutions obtained with *Mode* – 3, *Mode* – 5 and *Mode* – 6 are of similar quality and yield similar model parameters. The results obtained with *Mode* – 6 are in good agreement with the atmospheric parameters determined from the spectra. The computed light curve is compared with the observations in Fig. 3. This solution indicates that the grazing eclipse, lasting about five hours, occurs in the V745 Cas system. In Fig. 4 we show the equipotential surfaces of both components for the light curve solution at the phases mid-primary and mid-secondary eclipses. In the middle of the figure the volumes of the stars are compared with the Roche lobes.

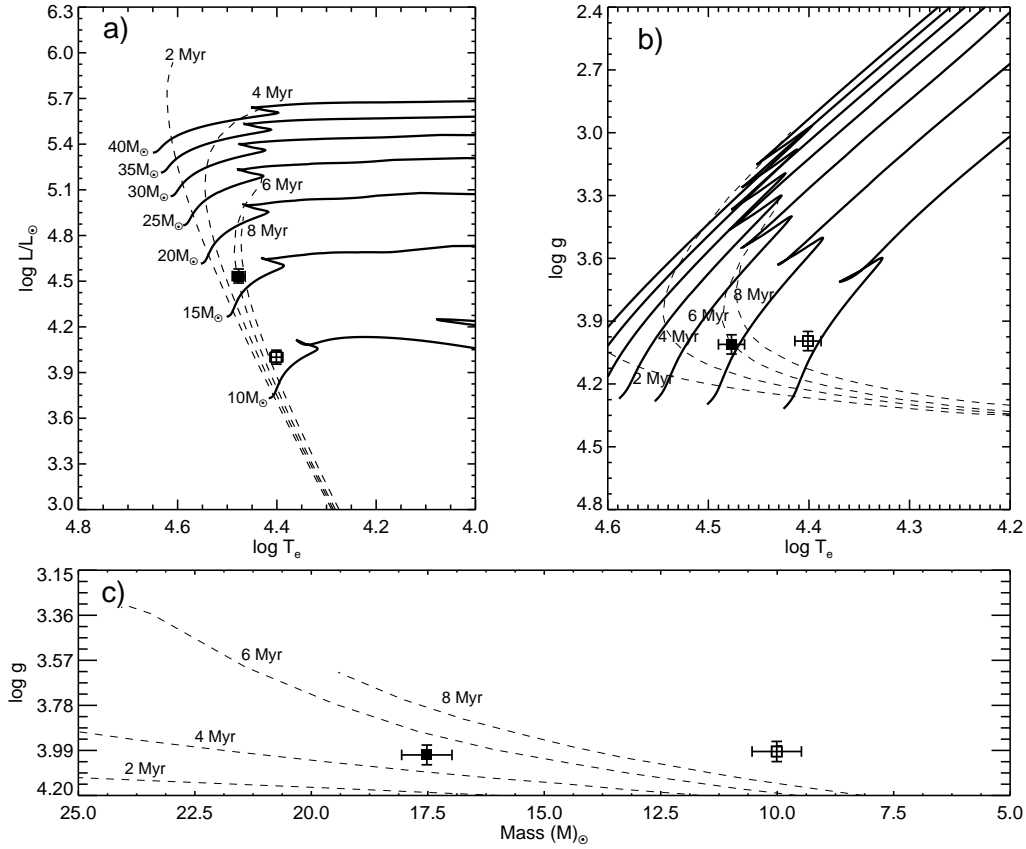


Figure 5. Positions of the components of the system in the luminosity-effective temperature and gravity effective temperature planes. The solid lines show evolutionary tracks for stars with masses of 40, 35, 30, 25, 20, 15 and 10 solar masses taken from Ekström et al. (2012).

5 RESULTS AND DISCUSSION

Combining the results of radial velocities and light curve analyses we have calculated the absolute parameters of the stars. Separation between the components of the eclipsing pair is calculated as $a=16.21\pm0.14R_{\odot}$. The fundamental stellar parameters for the components such as masses, radii, luminosities are listed in Table 5 together with their formal standard deviations. The standard deviations of the parameters have been determined by means of the JKTABSDIM³ code (Southworth et al. 2005). The mass for the primary of $M_p=18.31\pm0.51 M_{\odot}$ and secondary of $M_s=10.47\pm0.28 M_{\odot}$ are consistent with B0 V and B(1-2) IV-V stars.

The bolometric magnitudes of the components are computed as -6.62 ± 0.14 and -5.35 ± 0.06 mag for the primary and secondary components taking the absolute bolometric magnitude of the Sun as 4.74. The bolometric corrections listed in Table 5 are taken from Lanz & Hubeny (2007) adopting $V_{tur}=2 \text{ km s}^{-1}$, and $[Z/Z_{\odot}]=1.0$ (solar metallicity) and the effective temperatures and the surface gravities of the components given in the table. Using the interstellar reddening of

³ This can be obtained from <http://http://www.astro.keele.ac.uk/~jkt/codes.html>

Table 5. Properties of the V745 Cas components

Parameter	Primary	Secondary
Mass (M_{\odot})	18.31 ± 0.51	10.47 ± 0.28
Radius (R_{\odot})	6.94 ± 0.07	5.35 ± 0.05
T_{eff} (K)	$30\,000 \pm 1000$	$25\,540 \pm 300$
$\log(L/L_{\odot})$	4.547 ± 0.056	4.040 ± 0.025
$\log g$ (cgs)	4.018 ± 0.006	4.002 ± 0.007
<i>Sp. Type</i>	B0V	B(1-2)IV-V
M_{bol} (mag)	-6.62 ± 0.14	-5.35 ± 0.06
BC (mag)	-2.98	-2.63
M_V (mag)	-3.64 ± 0.14	-2.72 ± 0.06
$(v \sin i)_{calc.}$ (km s^{-1})	184 ± 2	142 ± 2
$(v \sin i)_{obs.}$ (km s^{-1})	171 ± 4	151 ± 8
d (pc)	$1\,703 \pm 63$	$1\,697 \pm 38$

$E(B-V)=0.34$ mag and absorption coefficient of 3.1 we estimate the absorption in visual band as 1.05 mag. With $V=8.18$ at the maximum light one finds $V_{0p}=7.52$ and $V_{0s}=8.43$ for the primary and secondary star, respectively. Then the distance modulus are 11.16 and 11.15 mag which correspond to the distances of $1\,703 \pm 63$ and $1\,697 \pm 38$ pc. As a weighted mean, we find the distance to the system as $1\,700 \pm 50$ pc.

Our line-of-sight passing through the binary system V745 Cas traverses first the *Perseus* arm of the *Galaxy* and then the distant *Cygnus* arm. The mean residual radial velocity and Galactocentric distance of the OB-associations in the *Perseus* region, including Cas OB4, were given as 8.4 kpc and -6.7 km s^{-1} . We estimated the distance of V745 Cas from the galactic plane as 20.4 pc and from galactic center as 8.5 kpc, where the distance of sun from the galactic plane is taken as 20.5 pc (Humphreys & Larsen 1995). The distances of the associations in the *Perseus* arm from the Sun were estimated between 1.8 and 2.8 kpc (Mel'nik & Dambis 2009). Therefore, we suspect that V745 Cas may be a member of the Cas OB4 association. If it is a member it should be located at the nearest edge of the association. This conclusion agrees with the result of Mel'nik & Efremov (1995) who quoted V745 Cas as a member of Cas OB4, for which they gave a distance of 2.04 kpc.

The distance to the Cas OB4 association had been subjected to various studies. There are a number of well-known OB associations and galactic open clusters in the direction of Cas OB4 association (approximately $l=120$, $b=0$ degrees). The mean interstellar reddening of 0.40, 0.34, 0.55, **0.47** and 0.55 mag, and distance of 1.43, 2.96, 3.8, 1.67 and 3.47 kpc were found for Mayer1 (Kharchenko et al. 2005), King 14 (Netopil et al. 2006), NGC 103 (Phelps & Janes 1993), NGC 129 (Turner et al. 1992) and NGC 146 (Subramaniam et al. 2005), respectively. The derived systemic velocity, reddening and distance of V745 Cas agree quite well with those values of NGC 129.

We have observed the components A, B, C and D of the multiple stellar system (WDS J00229+6214) simultaneously using the 100 cm telescope of the Turkish National Observatory of Turkey. We

Table 6. UBV measurements of the components B, C and D of the multiple stellar system and their probable spectral types.

Star	U	B	V	Q	Sp.Type
<i>B</i>	10.82	11.32	11.25	-0.542	B3
<i>C</i>	13.47	13.54	13.33	-0.218	B8
<i>D</i>	12.62	12.65	12.18	-0.357	B7

used the A-star as a reference for which UBV magnitudes are known. The photometric observations were made when the component A was at maximum light. The wide-band UBV magnitudes of the components B, C and D were obtained with respect to the component A and are presented in Table 6. The standard deviations of the measurements are about 0.01 mag. The apparent visual magnitude for C-star with a separation of 23.2 arcsec was given in the WDS catalogue as 10.8 which is inconsistent with that we determined. We suspect that the C-star may be variable in brightness. Using the Johnson Q–method we determined the spectral types of the stars as B3, B8 and B7 for B, C and D, respectively. According to this classification the interstellar reddening for B and C is similar with that of the eclipsing pair. However the D star appears to have the largest reddening, amounting to $E(B-V)=0.60$ mag. Such a result is expected because the reddening may vary from region to region in the association depending on the density of molecular clouds.

Figure 5 shows the components, with $1\text{-}\sigma$ error bars, of V745 Cas in the $\log T_{eff}\text{-}\log L/L_{\odot}$ (left panel) and $\log T_{eff}\text{-}\log g$ planes (right panel). The evolutionary tracks and isochrones for the non-rotating single stars with solar composition are taken from Ekström et al. (2012). The models considering mass loss and convective overshooting are adopted. We typically compare the positions of the stars with evolutionary tracks and determine what masses they would predict. This comparison points out a mass slightly smaller for the primary but higher for the secondary. The locations of the components in both panels show that the components are in the main sequence band, not far from the ZAMS. Although both components are young they fill their corresponding Roche lobes due to very small separation. Therefore, one should not necessarily expect a good agreement with single star tracks.

V745 Cas is one of a few massive contact binaries, namely TU Mus, V382 Cyg, and LY Aur (Penny et al. 2008). The masses of the components as well as the orbital period are very similar to that of TU Mus. As pointed out by Penny et al. (2008) the observed mass ratios of the contact systems are slightly higher than those of the semi-detached systems. The components of the contact systems have similar spectral types (within one spectral type of each other) and luminosity classes. Wellstein et al. (2001) presented evolutionary calculations for 74 systems considering case A and B scenarios. Our analyses indicate that V745 Cas is a contact system. Both components have nearly the same luminosity class and almost identical surface gravities, as given in

Table 5. Therefore, the system is most probably undergoing *case A* evolution. According to the Wellstein et al. (2001) models, *case A* contact systems can occur when the initial period of the system is very small and/or mass ratio is either very small or very large. The observed properties of the components are similar with those of the system No.53, (initial masses of 16 and 12 M_{\odot} and orbital period of 1.5 days) in their Table 3. Their model shows that the more massive star reaches its Roche lobe fairly early in its evolution. Rapid mass transfer from the more massive star to the less massive star occurs, the orbital period decreases which causes the loser star to overflow at a faster rate. Large increase in mass of the gainer star and smaller orbit cause it to expand and reach its *Roche* lobe. The orbit of the binary continues to shrink until the gainer star is more massive. Then the mass transfer after this point causes the orbit to expand, leading to a longer orbital period. Fast *case A* mass transfer still continues until the loser is much less massive. Since the ratio of mass in the core to that of the envelope of the loser is increasing this causes its radius to increase. Finally the gainer expands and reaches to the Roche lobe due to the increase in mass. Thus a contact system, similar to V745 Cas, is formed.

In Fig. 6 we show the correlations between luminosity-effective temperature, mass-luminosity, mass-radius and mass-effective temperature for the components of the detached massive eclipsing binaries where the filled circles refer to the primaries and the open circles to the secondaries. The parameters are taken from Torres et al. (2010). These stars lie close to the zero-age main-sequence on the HR diagram. Though the sample contains only ten stars reliable correlations between the parameters could be obtained. Linear least-squares fit to the data gives following relationships,

$$\log \frac{L}{L_{\odot}} = 7.34(\pm 0.60) \log T_{eff} - 28.48(\pm 2.69) \quad (2)$$

$$\log \frac{L}{L_{\odot}} = 3.07(\pm 0.17) \frac{M}{M_{\odot}} + 0.84(\pm 0.19) \quad (3)$$

$$\log T_{eff} = 0.39(\pm 0.02) \log \frac{M}{M_{\odot}} + 4.01(\pm 0.03) \quad (4)$$

$$\log \frac{R}{R_{\odot}} = 0.75(\pm 0.10) \log \frac{M}{M_{\odot}} - 0.08(\pm 0.11) \quad (5)$$

The numbers in the parentheses are the standard errors of the preceding coefficients determined by linear least squares solutions. The components of V745 Cas and MY Ser are shown by squares (primary:filled, secondary:empty) and triangles (primary:filled, secondary:empty) in Fig. 5. While the parameters for V745 Cas are determined in this study, the parameters for the components of MY Ser are adopted from Ibanoglu et al. (2013). The positions of the components of V745 Cas agree well with those of the components of detached, young massive eclipsing binaries. This may

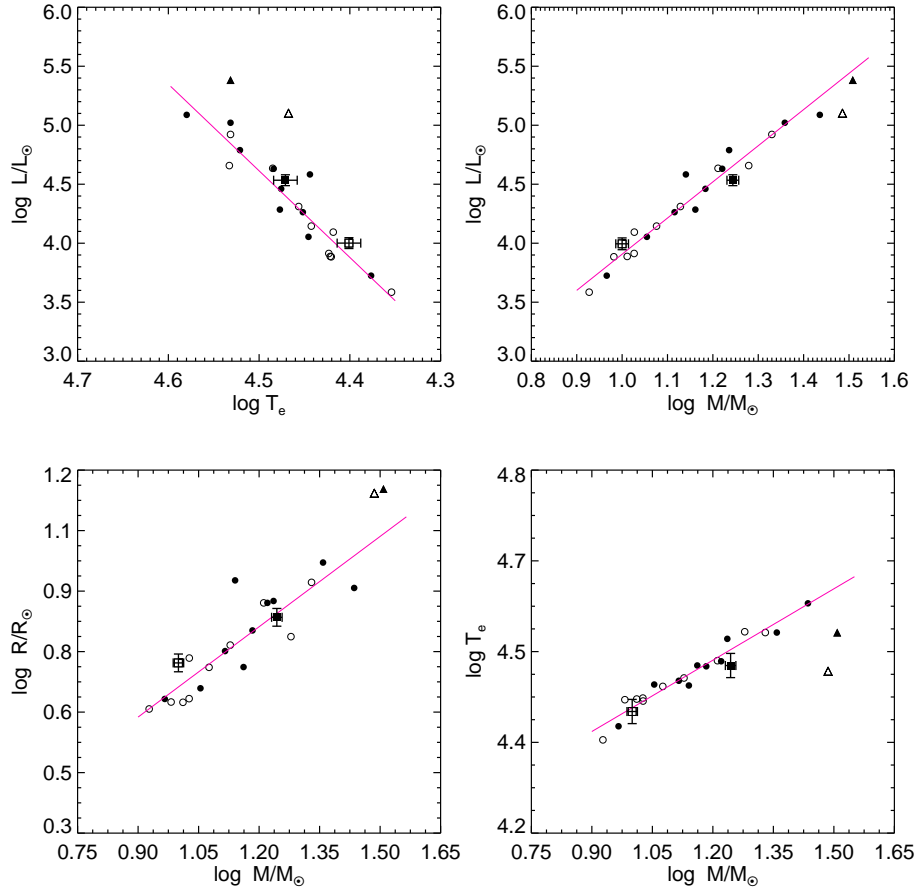


Figure 6. Locations of the primary (solid dots) and secondary (open circles) components of the detached, young eclipsing binary systems in various diagrams. (a) $\log L - \log T_{eff}$, (b) $\log L - \log M$, (c) $\log T_{eff} - \log M$ and (d) $\log R - \log M$. The solid lines show the best correlations between the parameters. The component of V745 Cas and MY Ser are shown by squares and triangles.

be taken as an indicator that mass-exchange between the components or mass-loss from them did not yet lead to a significant change on their radii and effective temperatures.

6 CONCLUSION

V745 Cas is one of the rare early type contact systems with massive components. Analysis of the radial velocities and light curves yielded absolute parameters of the components. The components are classified as B0V and B(1-2)V spectral types with masses of 18.31 ± 0.51 and $10.47 \pm 0.28 M_{\odot}$. Comparison with the evolutionary models and with the parameters of detached massive binaries show that both components are still close to the zero-age main-sequence. Although the components of V745 Cas are in contact with their Roche lobes they locate on the main-sequence band. Using our estimation of $E(B-V)$ and A_v we determined a distance of about 1700 ± 50 pc which is in agreement with the distance estimations of the Cas OB4 association. We also observed V745 Cas, the brightest component of the multiple star system with the other components simultaneously.

These observations indicate that the components B, C and D are also massive stars with spectral types of B3, B8 and B7.

ACKNOWLEDGMENTS

We thank to TÜBİTAK National Observatory (TUG) for a partial support in using RTT150 telescope with project number 11BRTT150-198. We also thank to the staff of the Bakırlitepe observing station for their warm hospitality. This study is supported by Turkish Scientific and Technology Council under project number 112T263. The following internet-based resources were used in research for this paper: the NASA Astrophysics Data System; the SIMBAD database operated at CDS, Strasbourg, France; and the arXiv scientific paper preprint service operated by Cornell University. This research was supported by the Scientific Research Projects Coordination Unit of Istanbul University. Project number 3685. We thank Çanakkale Onsekiz Mart University Astrophysics Research Center and Ulupınar Observatory together with İstanbul University Observatory Research and Application Center for their support and allowing use of IST60 telescope. The authors thank to the anonymous referee for helpful comments that improved the clarity of the text.

REFERENCES

- Abt, H. A., Levato, H., & Grosso, M. 2002, *ApJ*, 573, 359
- Alfonso-Garzón, J., Domingo, A., & Mas-Hesse, J. M., 2013, arXiv:1302.6898
- Alfonso-Garzón, J., Domingo, A., Mas-Hesse, J. M., & Giménez, A., 2012, *A&A*, 548, A79
- Conti, P. S., & Ebbets, D. 1977, *ApJ*, 213, 438
- Conti P. S., Garmany C. D., Massey P., 1986, *AJ*, 92, 48
- Cutri R. M., et al., 2003, The IRSA 2MASS All-Sky Point Source Catalog, NASA/IPAC Infrared Science Archive. <http://irsa.ipac.caltech.edu/applications/Gator/>
- Domingo, A., Caballero, M. D., Figueras, F., et al. 2003, *A&A*, 411, L281
- Drilling J. S., Landolt A. U., 2000, *Allen's astrophysical quantities*, 4th ed. Edited by Arthur N. Cox. ISBN: 0-387-98746-0. Publisher: New York: AIP Press; Springer, p.381
- Ekström S., Georgy C., Eggenberger P., et al., 2012, *A&A*, 537, A146
- Evans D. S., 1967, *IAUS*, 30, 57
- Frasca, A., Guillout, P., Marilli, E., et al. 2006, *A&A*, 454, 301
- Garmany, C. D., & Stencel, R. E., 1992, *AAPS*, 94, 211
- Gies, D. R., 2003, *IAUS*, 212, 91

- Guetter H. H., 1974, *PASP*, 86, 795
- Gray, D. F. 1976, *The observation and analysis of stellar photospheres*, (1st ed. New York: Wiley)
- Gray, D. F. 1992, *The observation and analysis of stellar photospheres*, (2nd ed.) *Camb. Astrophys. Ser.*, Vol. 20
- Harmanec, P. 1998, *A&A*, 335, 173
- Haug U., 1970, *A&AS*, 1, 35
- Hilditch, R. W., Howarth, I. D., & Harries, T. J., 2005, *MNRAS*, 357, 304
- Hovhannessian R. K., 2004, *Ap*, 47, 499
- Humphreys R. M., 1978, *ApJS*, 38, 309
- Humphreys, R. M., & Larsen, J. A., 1995, *AJ*, 110, 2183
- Ibanoglu, C., Cakırlı, Ö., & Sipahi, E., 2013, *MNRAS*, (in press)
- Johnson H. L., Morgan W. W., 1953, *ApJ*, 117, 313
- Kane S. R., Schneider D. P., Ge J., 2007, *MNRAS*, 377, 1610
- Kazarovets E. V., Samus N. N., Durlevich O. V., et al., 1999, *IBVS*, 4659, 1
- Kharchenko, N. V., Piskunov, A. E., Röser, S., Schilbach, E., & Scholz, R.-D., 2005, *A&A*, 438, 1163
- Kurucz, R. L., & Avrett, E. H., 1981, *SAO Special Report*, 391,
- Lanz, T., & Hubeny, I., 2007, *ApJS*, 169, 83
- Lenz, P., & Breger, M., 2005, *Communications in Asteroseismology*, 146, 53
- Massey, P., Morrell, N. I., Neugent, K. F., et al., 2012, *ApJ*, 748, 96
- Meisel, D. D. 1968, *AJ*, 73, 350
- Mel'nik A. M., Dambis A. K., 2009, *MNRAS*, 400, 518
- Mel'nik A. M., Efremov Y. N., 1995, *AstL*, 21, 10
- Moe, M., & Di Stefano, R., 2013, *ApJ*, 778, 95
- Morgan W. W., Whitford A. E., Code A. D., 1953, *ApJ*, 118, 318
- Netopil, M., Maitzen, H. M., Paunzen, E., & Claret, A., 2006, *A&A*, 454, 179
- Penny, L. R. 1996, *ApJ*, 463, 737
- Penny, L. R., Ouzts, C., & Gies, D. R. 2008, *ApJ*, 681, 554
- Perryman M. A. C., Lindegren L., Kovalevsky J. et al., 1997, *A&A*, 323, L49
- Petrie R. M., Pearce J. A., 1961, *PDAO*, 12, 1
- Phelps, R. L., & Janes, K. A., 1993, *AJ*, 106, 1870
- Prša A., Zwitter T., 2005, *ApJ*, 628, 426P
- Reed B. C., 2003, *AJ*, 125, 2531

- Royer F., Gerbaldi M., Faraggiana R., & Gomez A. E., 2002, *A&A*, 381, 105
- Sana, H., de Koter, A., de Mink, S. E., et al., 2013, *A&A*, 550, A107
- Sanford R. F., Merrill P. W., 1938, *ApJ*, 87, 517
- Simkin S. J., 1974, *A&A*, 31, 129
- Simón-Díaz, S., & Herrero, A. 2014, *AA*, 562, A135
- Southworth J., Smalley B., Maxted P. F. L., Claret A. & Etzel P. B., 2005, *MNRAS*, 363, 529
- Subramaniam, A., Sahu, D. K., Sagar, R., & Vijitha, P., 2005, *A&A*, 440, 511
- Tonry, J., & Davis, M. 1979, *AJ*, 84, 1511
- Torres G., Andersen J., & Giménez A., 2010, *A&ARv*, 18, 67
- Turner, D. G., Forbes, D., & Pedreros, M., 1992, *AJ*, 104, 1132
- van der Hucht K. A., 1996, *LIACo*, 33, 1
- Valdes, F., Gupta, R., Rose, J. A., Singh, H. P., & Bell, D. J., 2004, *ApJS*, 152, 251
- van Hamme, W., 1993 *AJ*, 106, 2096
- van Leeuwen, F. 2007, *A&A*, 474, 653
- Wellstein, S., Langer, N., & Braun, H. 2001, *A&A*, 369, 939
- Wilson, R. E., 1953, Carnegie Institute Washington D.C. Publication
- Wilson, R. E., 2006, *Astrophysics of Variable Stars*, ASPC, 349, 71
- Wilson, R. E., & Devinney, E. J. 1971, *ApJ*, 166, 605
- Wu, Y., Singh, H. P., Prugniel, P., Gupta, R., & Koleva, M. 2011, *A&A*, 525, A71